JMEPEG (2018) 27:1628–1634
https://doi.org/10.1007/s11665-018-3268-z

1059-9495/$19.00

Effect of Retrogression Heat Treatment Time on Microstructure and Mechanical Properties of AA7010

M.S. Nandana, K. Udaya Bhat, and C.M. Manjunatha

(Submitted August 29, 2017; in revised form December 28, 2017; published online March 6, 2018)

The effect of retrogression time during retrogression and re-aging (RRA) treatment of AA7010 is evaluated by performing tensile tests and characterizing the microchemistry of the grain boundary precipitates (GBPs) using transmission electron microscope coupled with the energy-dispersive spectroscopy. Retrogression time is evaluated so that the ultimate tensile strength of the RRA-treated sample is equal to that of the T6-treated sample and the grain boundary microstructure similar to that of the over-aged (T7451) condition. The investigation reveals that the sample retrogressed at 200 °C for 20 min has UTS of 586 MPa which is equivalent to that of the T6 sample and 11.5% higher than that of the T7451 condition. The fracture toughness of the RRA-treated sample was 41 MPa$\sqrt{m}$. Microstructure of the RRA-treated sample is similar to T7451, along the grain boundaries and in the grain interior similar to that of the T6-treated sample. Energy-dispersive spectroscopy confirmed the increment of Cu content on the GBP's with increase in the retrogression time, which is expected to improve the stress corrosion cracking resistance of the alloy.

Keywords fracture toughness, GBP, peak aging, RRA, SCC, TEM

1. Introduction

The 7xxx series aluminum alloys are extensively used in the aerospace structural applications, such as lug joints and bulk heads (Ref 1-3) due to their good specific strength and damage tolerance behavior (Ref 4). They are generally used in T6 heat-treated condition which ensures good strength. In several applications, such as military and naval aircrafts, these alloys are exposed to corrosive environment in addition to loads. Under these environmental conditions, the presence of different intermetallic particles in these alloys, which exhibit different electrochemical potential with the grain interior, leads to the formation of corrosion pits (Ref 2). With the application of the load, pits act as stress raisers leading to stress corrosion cracking (SCC) (Ref 5). Thus, the stress corrosion cracking behavior of these alloys assumes significant importance in these materials.

Although 7xxx series aluminum alloys exhibit high strength in T6 heat-treated condition, they possess poor resistance to SCC. In order to overcome the stress corrosion cracking susceptibility, these alloys are used in T7 condition (Ref 2). The size and distribution of the grain boundary precipitates get modified during T7 heat treatment, and it makes them more resistant to SCC. The SCC resistance is imparted due to the change in microchemistry and chemical activity of grain boundary precipitates. These precipitates are generally anodic with the grain interior in the aluminum alloys containing more than 1% Cu (Ref 6, 7). However, T7 heat treatment has been observed to reduce the strength by 10-15%, resulting in added weight penalty to the structural components (Ref 8). A new heat treatment called retrogression and re-aging (RRA) has been proposed which imparts the alloy with the mechanical properties equivalent to T6 and SCC resistance equivalent to T7 heat-treated alloy (Ref 9).

The precipitation sequence in Al-Zn-Mg-Cu alloy is as following (Ref 10):

$$\text{Supersaturated solid solution} \rightarrow \text{Vacancy rich clusters} \rightarrow \text{GP zones} \rightarrow \eta' \rightarrow \eta(MgZn_2)$$

The RRA heat treatment involves an additional heat treatment of T6-treated alloy to a higher temperature range between 180 and 250 °C and re-aging to peak aging condition. The mechanical and corrosive properties of the material depend on the temperature and time of the reversion and re-aging steps. The recent investigations on RRA treatment of aluminum alloys have shown that the grain size and grain boundary microstructures influence the fatigue fracture behavior. The fracture behavior is influenced by the strength difference between the grain interior and the grain boundary. The T761-tempered alloy exhibited intergranular crack during fatigue, due to the formation of the wider precipitate free zone (PFZ). In contrast, there exist both intergranular and transgranular fractures in the RRA-treated condition which is beneficial in retarding fracture tendency (Ref 11).

AA7010 is one of the ultra-high-strength wrought aluminum alloys, used in the aircrafts primary structural applications where strength is the limiting design parameter. It is well known that RRA is established to retain the peak strength of the alloy along with SCC resistance similar to that of over-aged condition (Ref 12). But optimization of the RRA treatment coupled with quantification of the microchemistry of the GBPs is not much reported. The aim of the present research work is to optimize the retrogression time at 200 °C retrogression temperature, so as to obtain equivalent tensile properties of T6-treated sample and to quantify the variation of the copper

M.S. Nandana and **K. Udaya Bhat**, Department of Metallurgical and Materials Engineering, National Institute of Technology Karnataka, Surathkal, India; **C.M. Manjunatha**, Structural Technologies Division, CSIR-National Aerospace Laboratories, Bangalore, India. Contact e-mails: nandanams88@gmail.com, udayabhatk@gmail.com, and manjucm@nal.res.in.

content in the GBPs. Along with the desired mechanical properties, the grain boundary characteristics are expected to be similar to that of the T7 (over-aged)-treated sample which is essential for improving the SCC resistance of the alloy.

2. Experimental Procedure

The material used for the present research work is commercial aluminum alloy 7010 received in rolled form in T7451 (over-aged) condition. The alloy composition is: Al-89.4, Zn-6.3, Mg-2.21, Cu-1.65, Zr-0.124, Fe-0.21 and Si-0.073 (in wt.%). The alloy is solution heat-treated at 490 °C for 6 h (optimized by experiments) and quenched in water maintained at room temperature. The quenched samples are then pre-aged at 120 °C for 24 h duration. Retrogression is performed by heat treating the pre-aged alloy to 200 °C for different time intervals and re-aging at 120 °C for 24 h. The retrogression temperature is selected based on the reported investigations (Ref 13, 14). The tempering designation for different heat treatments performed is listed in Table 1. The optimization of the retrogression time is obtained by conducting tensile tests. The typical heat treatment procedure for RRA is shown in Fig. 1.

Tensile tests were performed in longitudinal direction as per ASTM E8, using universal testing machine (UTM, Shimadzu make, model: AG-X plus) of 100 kN capacity. During this, crosshead speed of 1 mm/min was maintained. Linear elastic fracture toughness tests were performed on the compact tension samples in L–T orientation, as per ASTM E399, to evaluate and compare the fracture toughness of the different heat-treated samples. Standard CT specimens with width of 50 mm and thickness of 25 mm were employed for evaluating the fracture toughness. Microhardness tests were performed using Vicker's microhardness instrument (Shimadzu make model: G21). Indentation load of 500 g was applied and time of indentation maintained for 15 s. The microstructural characterization of the heat-treated samples was done by using TEM (make JEOL, JEM-2100), operating at an accelerating voltage of 200 kV. Fractured surfaces were analyzed using secondary electron imaging mode in scanning electron microscope (JSM 6380 LA, JEOL make).

3. Results and Discussion

3.1 Microstructural Characterization

The bright-field TEM micrographs of the alloy samples heat-treated to T6, retrogressed at 200 °C for 20 min, RRA, and T7451 are produced in Fig. 2. Figure 2(a) shows the matrix

Table 1 Heat treatment steps adopted for AA7010

Tempering designation	Heat treatment description (measuring error ± 2 °C)
T6	490 °C for 6 h + water quench + 120 °C for 24 h
RRA	490 °C for 6 h + water quench + 120 °C for 24 h + 200 °C for 20 min + 120 °C for 24 h
T7451	490 °C for 6 h + water quench + 115 °C for 8 h + 165 °C 16 h

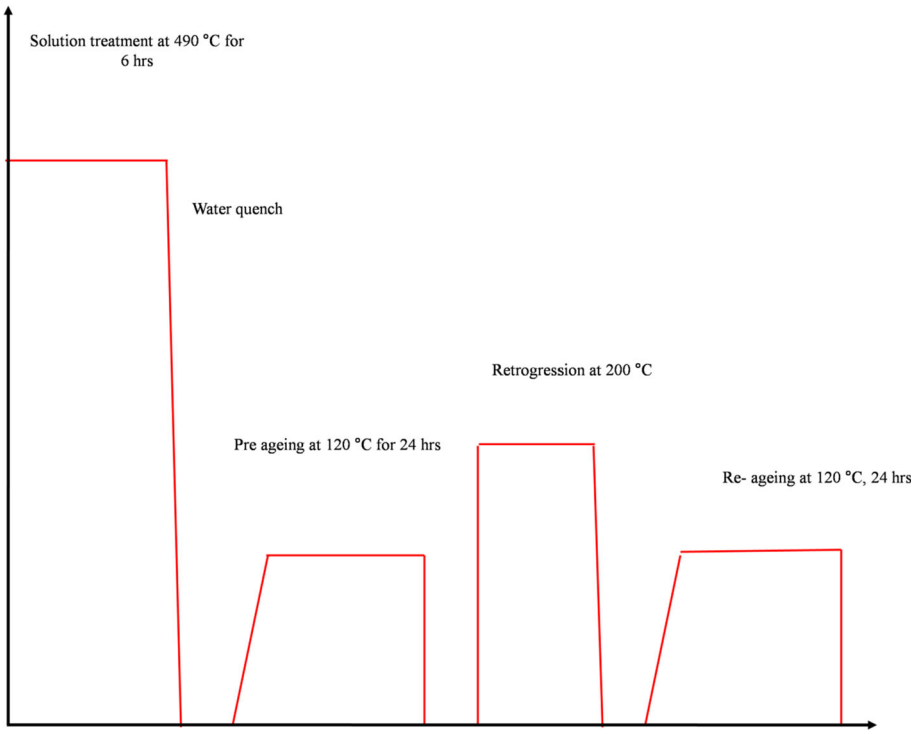

Fig. 1 Schematic representation of retrogression and re-aging treatment

of T6-treated alloy dispersed with the GP zones and fine-scale metastable precipitates η' ($MgZn_2$) of size varying from 3 to 5 nm, which is similar to the values reported by earlier researchers (Ref 15, 16). The grain boundary precipitates (Fig. 2b) in T6 condition are thin and continuous. During retrogression, unstable GP zones are completely dissolved and metastable η' precipitates get partially dissolved (Ref 17). This is evident from the reduced density of the fine-scale precipitates, as observed in bright-field TEM micrographs of the retrogressed sample (Fig. 2c, d). When these retrogressed samples are re-aged to peak aging condition, the partially dissolved η' precipitates will grow further to become elongated disks of size (10-12 nm) and transform into stable η precipitates. The GP zones and η' precipitates dissolved during retrogression will reprecipitate during re-aging. The η' precipitates (4-5 nm) as observed by the diffused spots at 1/3 and 2/3 of 220_{Al} position in $[111]_{Al}$ (Fig. 3a), which is responsible for imparting the strength characteristics of T6-treated sample (Ref 16). The grain boundary precipitate η gets coarsened and becomes discontinuous with size (25-50 nm) during re-aging (Ref 18) as shown in Fig. 2(f). Figure 3(b) represents $[122]_{Al}$ SAED pattern highlighting the diffused ring corresponding to the presence of η precipitates. The GBPs are more widely spaced with the average interspacing of 24 nm. The width of the PFZ is found to vary from 35 to 38 nm which is slightly higher than that of the T6-treated sample. The size of the precipitates with different morphologies and PFZ width in different heat-treated samples are quantified and pictorially represented in Fig. 4(a).

In T7451 (over-aged) condition shown in Fig. 2(g, h), the grain interior is occupied with lesser dense η' precipitates of size (8-12 nm). The grain interior is majorly occupied with elongated disks (η precipitates) of size (20-45) nm. The average GBPs size and PFZ width are 60 nm and 70 nm, respectively. The T6-treated alloys are more prone to SCC. The grain boundary precipitates in T6 act anodic with the grain interior forming active galvanic cell path leading to corrosion of grain boundaries (Ref 19). The presence of continuous grain boundary precipitates in the case of T6-treated condition further promotes intergranular crack path (Ref 20).

The recent researches have shown that the size, Cu content and interspacing of GBPs play a major role in controlling the SCC, in high-strength aluminum alloys (Ref 13). With the increase in aging temperature, more Cu is diffused into the grain boundaries. The TEM–EDS is used for characterizing the microchemistry of the grain boundary precipitates in RRA-treated samples with retrogression performed for different time intervals (10-60 min). It is evident from the EDS analysis that GBPs are increased with the Cu content as retrogression time is increased. The average Cu content of GBPs quantified by EDS is represented in Fig. 4(b). The GBPs of T6-treated alloy contains 2.52 (wt.%) of Cu. In contrast, GBPs of RRA-treated samples contained Cu in the range of 4.04 (Fig. 5) to 5.27 (wt.%), for 20 and 60 min retrogression periods, respectively. The Cu content of 60-min retrogressed and re-aged sample is higher than that of the over-aged sample (4.81 wt.%). The GBPs with increased Cu content lead to the reduction in electrochemical potential difference between the grain interior and the grain boundary region. It accounts for better stress corrosion cracking resistance of the alloy. It is expected that increased Cu content at the grain boundary region during retrogression would delay the corrosion attack on the GBPs. The discontinuous GBPs would further resist the SCC. The microstructure of the RRA-treated condition exhibits similar characteristics of T7 condition along the grain boundaries, and similar characteristics of T6 condition, in the matrix. This is expected to provide enhanced SCC resistance along with the tensile properties equivalent to that of the T6-treated condition.

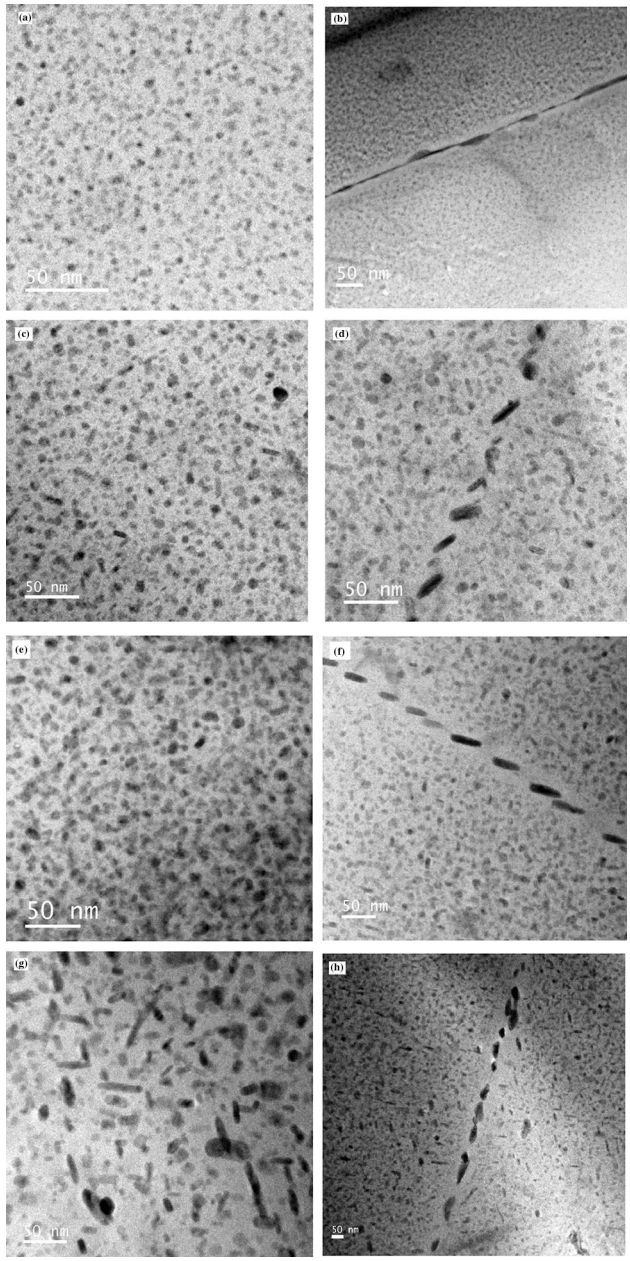

Fig. 2 Bright-field TEM micrographs of the AA7010 on the matrix and grain boundary at different aging conditions; (a, b) T6, (c, d) retrogression at 200 °C for 20 min, (e, f) RRA 200 °C at 20 min, (g, h) T7451 as-received

3.2 Tensile Test

Figure 6(a) compares the results of the tensile tests performed on RRA heat-treated samples. The yield strength, UTS

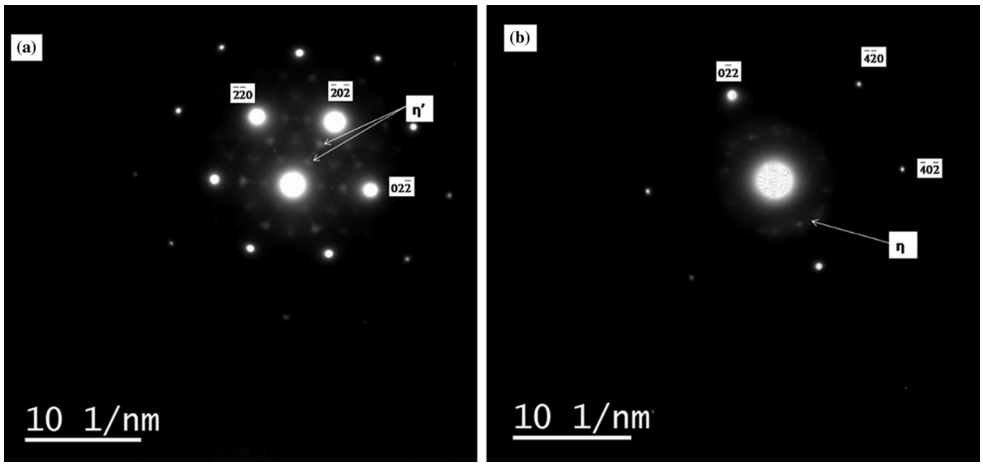

Fig. 3 (a) $[111]_{Al}$ SAED pattern indicating η' precipitate at 1/3 and 2/3 of 220_{Al} position; (b) $[122]_{Al}$ SAED pattern with diffused ring corresponding to η precipitate

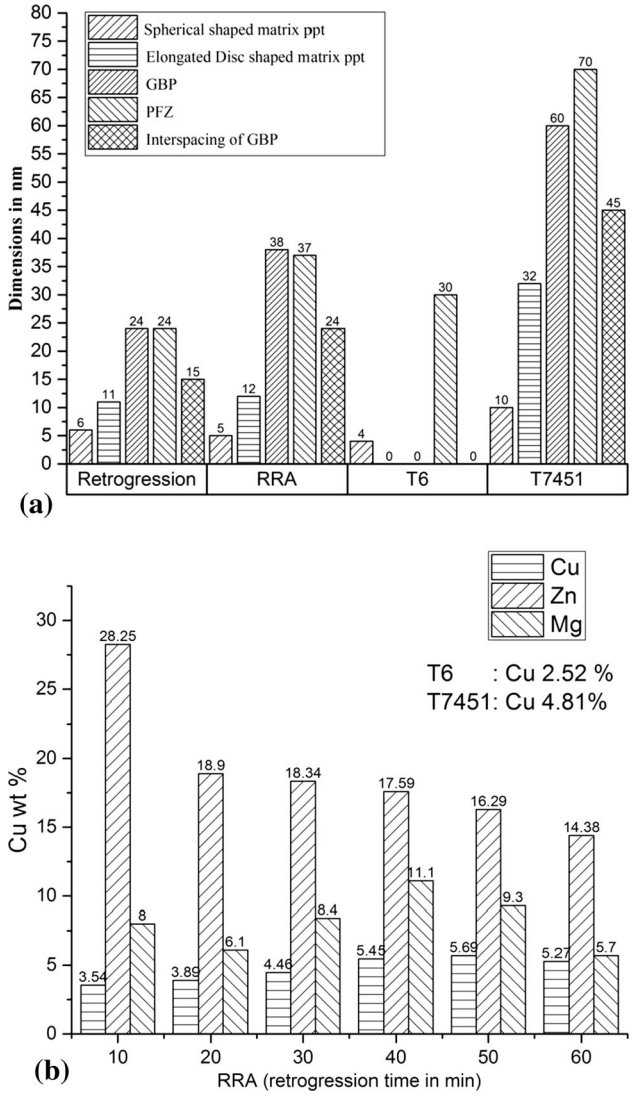

Fig. 4 (a) Precipitate size in the matrix, grain boundary, PFZ size and spacing of GBP's. (b) Variation of Cu (wt.%) on the GBP's

and % elongation to fracture are plotted for RRA-treated samples, corresponding to retrogression done for different time intervals at 200 °C. A maximum strength of 609 MPa is obtained for short time retrogression performed for 5 min. With the retrogression time increased, continuous drop in both yield strength and UTS is observed which is due to the coarsening of precipitates in the matrix. The microhardness plot in Fig. 6(b) also demonstrates the similar behavior of drop in hardness with retrogression time. To acquire the high strength equivalent to that of T6 and grain boundary microstructure similar to that of T7451, retrogression at 200 °C for 20 min is considered as optimized condition. A representative stress vs strain plot comparing the deformation behavior of different heat-treated samples is shown in Fig. 7(a). The optimized RRA resulted in the UTS of 586 MPa, which is slightly higher and equivalent to T6-treated condition. Apart from the equivalent UTS, the RRA-treated samples also exhibited 6% higher in the yield strength. The yield strength of the RRA- and T6-treated samples is 514 and 486 MPa, respectively. It is also noted that optimized RRA did not loose much ductility and % elongation to fracture stood at 11.3%. Figure 7(b) compares the YS, UTS and % elongation of T6, T7451 and RRA (retrogression for 20 min) conditions. The tensile fracture surfaces of T7451-treated sample exhibited both intergranular and transgranular fracture, whereas T6- and RRA-treated samples exhibited dimples indicating ductile fracture. This is shown in the fractographs in Fig. 8.

3.3 Fracture Toughness Test

The fracture toughness of the T7451-, RRA- and T6-treated samples stood at 40, 41 and 42 MPa$\sqrt{m}$, respectively. Three trials were performed for each heat-treated conditions, and a standard deviation of 2, 1.5 and 2 was observed for T7451-, RRA- and T6-treated samples, respectively. The increased PFZs weaken the grain boundary and promote intergranular crack growth during fracture (Ref 21). RRA-treated samples with narrow PFZ, coarsened GBPs and grain interior similar to T6 lower the strength difference between the grain interior and grain boundary and thereby promotes microvoid coalescence of the matrix that leads to transgranular fracture (Ref 22).

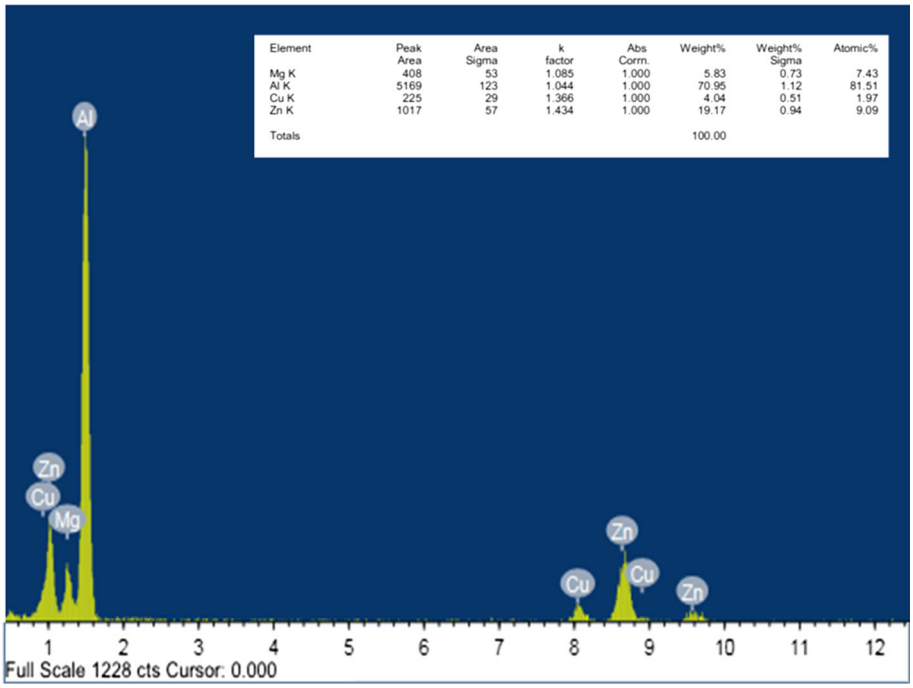

Fig. 5 Chemical composition of the GBPs analyzed by TEM–EDS for RRA 20 min condition

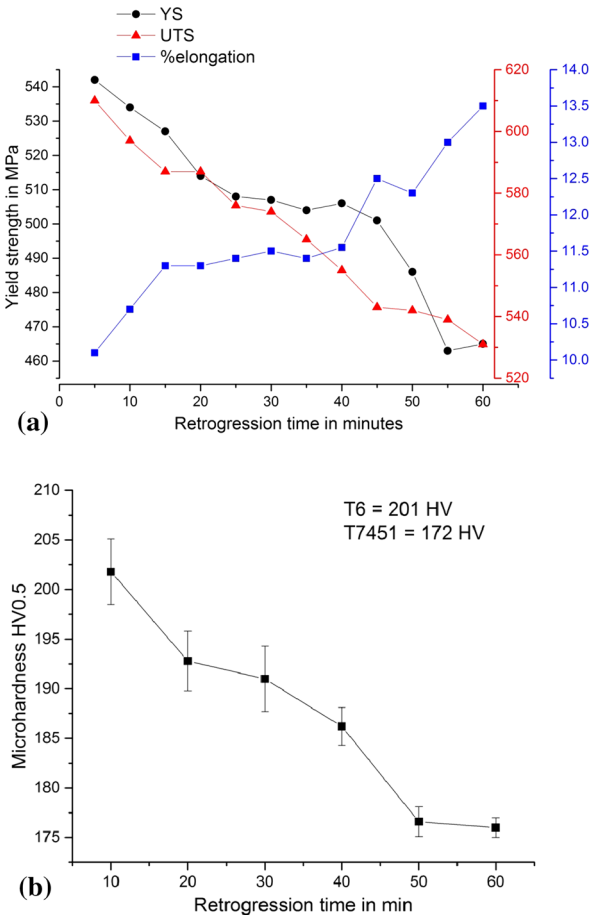

Fig. 6 (a) YS, UTS and % elongation of AA7010 heat-treated to RRA: retrogression performed for different time intervals. (b) Microhardness data measured on RRA samples with different retrogression duration

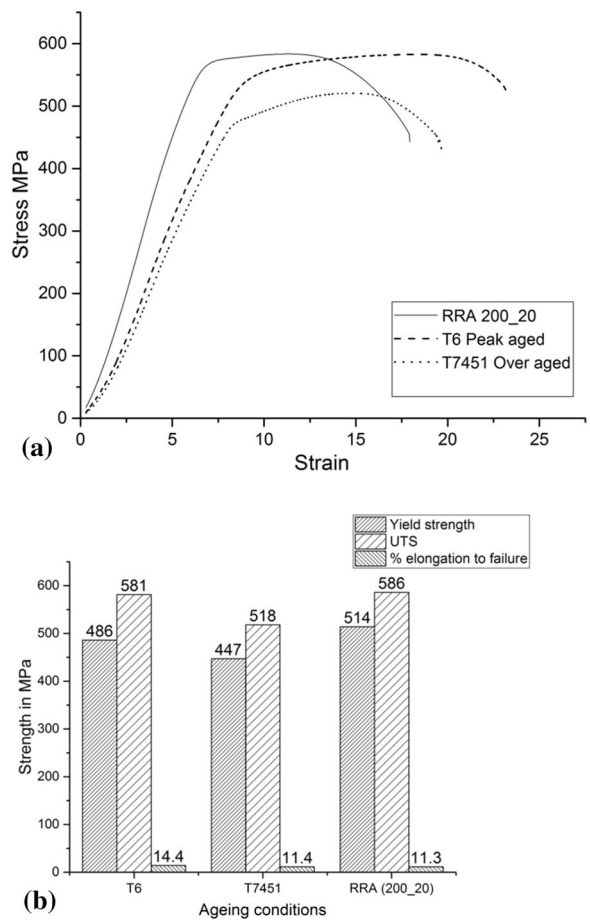

Fig. 7 (a) Stress vs. strain plot for AA7010 at different tempering conditions. (b) Comparison of YS, UTS and % elongation of alloy in different tempering conditions

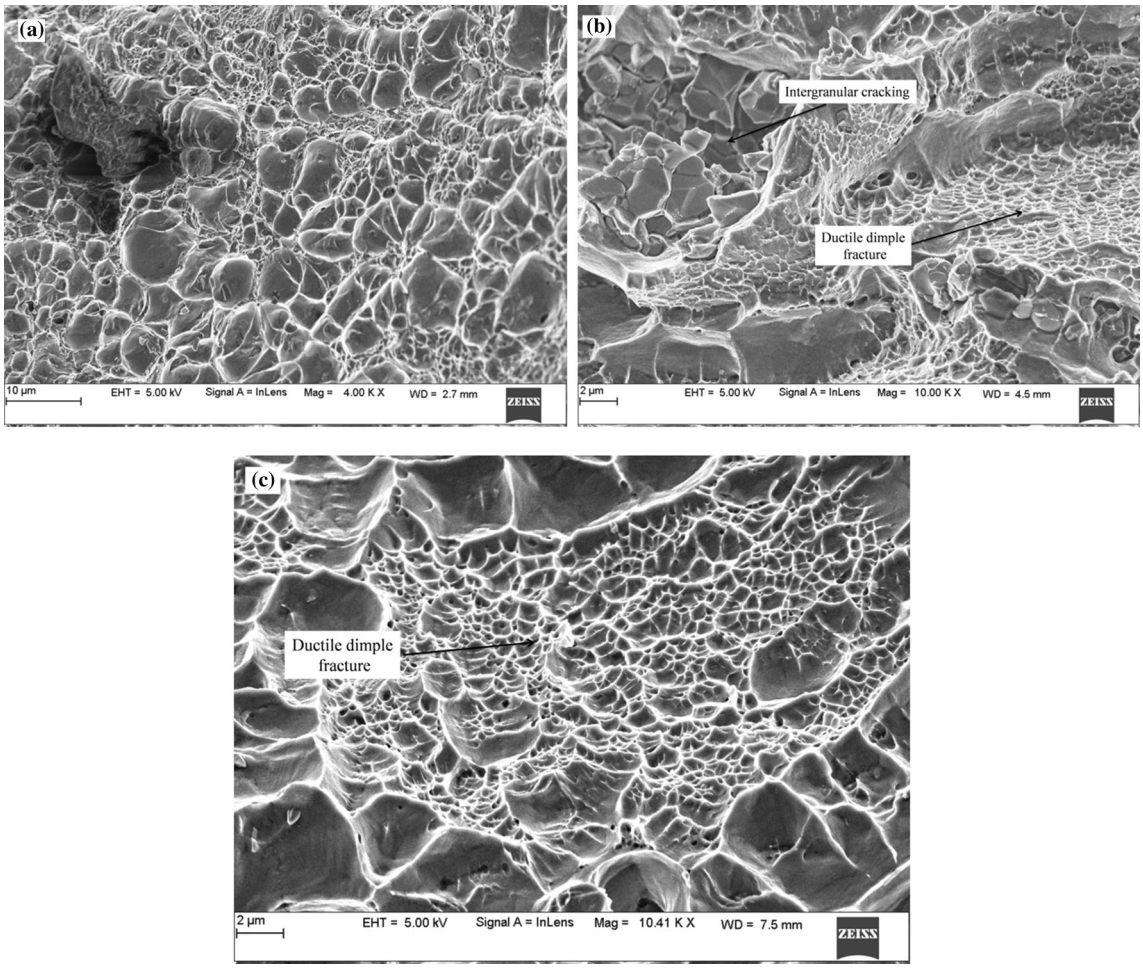

Fig. 8 Fractographs of AA7010 at different aging conditions: (a) T6, (b) T7451, (c) RRA

4. Conclusions

1. The matrix of the RRA-treated alloy is majorly populated with denser η' precipitates and fewer elongated disk-shaped η precipitates compared to T6-treated sample. The GBPs are coarsened, and grain boundary microstructure is closer to that of the T7451 condition. Narrowed PFZ is observed in the RRA-treated sample compared to T7451-treated condition, which is beneficial from the fracture perspective.
2. Significant improvement in the Cu content of GBPs of about 54% compared to T6 could be achieved by retrogressing for 20 min and re-aging. This behavior is expected to improve the corrosion resistance of the alloy compared to the T6-treated condition.
3. Retrogression performed at 200 °C for 20 min resulted in the equivalent mechanical properties of the T6 and similar grain boundary characteristics as that of the T7451 condition.
4. The fracture toughness of the RRA-treated sample is also equivalent to that of the over-aged (T7451) sample.
5. The PFZ size of RRA-treated sample is narrow compared to T7451 condition, which will promote transgranular fracture mode.

Acknowledgments

Authors are thankful to The Director, NITK, and The Director, CSIR-NAL, for facilitating to conduct this research work and also for their continuous encouragement. One of the authors Mr. Nandana would like to thank the MHRD-Government of India for providing the scholarship grant. The technical staff at the Department of Metallurgical and Materials Engineering, NITK, is thanked for their support.

References

1. Y.L. Wu, F.H. Froes, A. Alvarez, C.G. Li, and J. Liu, Microstructure and Properties of a New Super-High-Strength Al-Zn-Mg-Cu Alloy C912, *Mater. Des.*, 1988, **18**, p 211–215
2. F. Viana, A.M.P. Pinto, H.M.C. Santos, and A.B. Lopes, Retrogression and Re-ageing of 7075 Aluminium Alloy: Microstructural Characterization, *J. Mater. Process. Technol.*, 1999, **92–93**, p 54–59
3. J. Schijve, Fatigue Damage in Aircraft Structures, Not Wanted, But Tolerated?, *Int. J. Fatigue*, 2009, **31**(6), p 998–1011
4. L.P. Borrego, J.M. Costa, S. Silva, and J.M. Ferreira, Microstructure Dependent Fatigue Crack Growth in Aged Hardened Aluminium Alloys, *Int. J. Fatigue*, 2004, **26**(12), p 1321–1331
5. M. Puiggali, A. Zielinski, J.M. Olive, E. Renauld, D. Desjardins, and M. Cid, Effect of Microstructure on Stress Corrosion Cracking of an Al-Zn-Mg-Cu Alloy, *Corros. Sci.*, 1998, **40**(4–5), p 805–819

6. H.L. Liao, J.C. Lin, and S.L. Lee, Effect of Pre-immersion on the SCC of Heat-Treated AA7050 in an Alkaline 3.5%NaCl, *Corros. Sci.*, 2009, **51**(2), p 209–216
7. M. Dixit, R.S. Mishra, and K.K. Sankaran, Structure Property Correlations in Al 7050 and Al 7055 High-Strength Aluminum Alloys, *Mater. Sci. Eng., A*, 2008, **478**, p 163–172
8. P. Rout, M. Ghosh, and K. Ghosh, Microstructural, Mechanical and Electrochemical Behavior of a 7017 Al-Zn-Mg Alloy of Different Tempers, *Mater. Charact.*, 2015, **104**, p 49–60
9. B. Cina, Reducing Stress Corrosion Cracking in Aluminium Alloys, U.S. Patent 3856584, 24 December 1974
10. H. Ji-Wu, W. Tao, Y. Zhi-Min, S. Kai, and L. Jie, Single Ageing Characteristics of 7055 Aluminium Alloy, *Trans. Nonferrous Met. Soc. China*, 2017, **17**, p 548–552
11. X. Chen, Z. Liu, M. Lin, A. Ning, and S. Zeng, Enhanced Fatigue Crack Propagation Resistance in an Al-Zn-Mg-Cu Alloy by Retrogression and Re-agieng Treatment, *J. Mater. Eng. Perform.*, 2012, **21**, p 2345–2353
12. J.S. Robinson, S.D. Whelan, and R.L. Cudd, Retrogression and Re-ageing of 7010 Open Die Forgings, *Mater. Sci. Technol.*, 2013, **15**(6), p 717–724
13. M. Angappan, V. Sampath, B. Ashok, and V.P. Deepkumar, Retrogression and Re-aging Treatment on Short Transverse Tensile Properties of 7010 Aluminium Alloy Extrusions, *Mater. Des.*, 2011, **32**, p 4050–4053
14. A.F. Oliveira, M.C. De Barros, K.R. Cardoso, and D.N. Travessa, The Effect of RRA on the Strength and SCC Resistance on AA7050 and AA7150 Aluminium Alloys, *Mater. Sci. Eng., A*, 2004, **379**, p 321–326
15. T. Marlaud, A. Deschamps, F. Bley, W. Lefebvre, and B. Baroux, Evolution of Precipitate Microstructures During the Retrogression and Re-ageing Heat Treatment of an Al-Zn-Mg-Cu alloy, *Acta Mater.*, 2010, **58**(14), p 4814–4826
16. J. Buha, R.N. Lumley, and A.G. Crosky, Secondary Ageing in an Aluminium Alloy 7050, *Mater. Sci. Eng., A*, 2008, **492**(1–2), p 1–10
17. C.F. Meng, H.W. Long, and Y. Zheng, A Study of the Mechanism of Hardness Change of Al-Zn-Mg Alloy During Retrogression Re-ageing Treatments by Small Angle X-Ray Scattering (SAXS), *Metall. Mater. Trans. A*, 1997, **28**(10), p 2067–2071
18. J.S. Robinson, Influence of Retrogression and Reaging on Fracture Toughness of 7010 Aluminium Alloy, *Mater. Sci. Technol.*, 2003, **19**(12), p 1697–1704
19. J.F. Li, N. Birbilis, C.X. Li, Z.Q. Jia, B. Cai, and Z.Q. Zheng, Influence of Retrogression Temperature and Time on the Mechanical Properties and Exfoliation Corrosion Behavior of Aluminium Alloy AA7150, *Mater. Charact.*, 2009, **60**(11), p 1334–1341
20. J.F. Li, Z.Q. Zheng, S.C. Li, W.J. Chen, W.D. Ren, and X.S. Zhao, Simulation Study on Function Mechanism of Some Precipitates in Localized Corrosion of Al Alloys, *Corros. Sci.*, 2007, **49**(6), p 2436–2449
21. P. Xia, Z. Liu, S. Bai, L. Lu, and L. Gao, Enhanced Fatigue Crack Propagation Resistance in a Super High Strength Al-Zn-Mg-Cu Alloy by Modifying RRA Treatment, *Mater. Charact.*, 2016, **118**, p 438–445
22. M.N. Desmukh, R.K. Pandey, and A.K. Mukhopadhyay, Effect of Aging Treatments on the Kinetics of Fatigue Crack Growth in 7010 Aluminum Alloy, *Mater. Sci. Eng., A*, 2006, **435–436**, p 318–326